WSTIAC
Weapon Systems Technology
Information Analysis Center

WSTIAC Quarterly
Volume 9, Number 3

SUGV Teleoperations

WSTIAC is a DoD Information Analysis Center Sponsored by the Defense Technical Information Center

http://wstiac.alionscience.com/quarterly

Report Documentation Page

Form Approved
OMB No. 0704-0188

1. REPORT DATE **01 JAN 2010**	2. REPORT TYPE **N/A**	3. DATES COVERED **-**

4. TITLE AND SUBTITLE **WSTIAC Quarterly, Vol. 9, No. 3 - SUGV Teleoperations**	5a. CONTRACT NUMBER 5b. GRANT NUMBER 5c. PROGRAM ELEMENT NUMBER
6. AUTHOR(S)	5d. PROJECT NUMBER 5e. TASK NUMBER 5f. WORK UNIT NUMBER
7. PERFORMING ORGANIZATION NAME(S) AND ADDRESS(ES) **WSTIAC Weapon Systems Technology Information Analysis Center, Rome, NY**	8. PERFORMING ORGANIZATION REPORT NUMBER **WSTIAC-V9-N3**
9. SPONSORING/MONITORING AGENCY NAME(S) AND ADDRESS(ES) **Defense Technical Information Center, Ft Belvoir, VA**	10. SPONSOR/MONITOR'S ACRONYM(S) 11. SPONSOR/MONITOR'S REPORT NUMBER(S)

12. DISTRIBUTION/AVAILABILITY STATEMENT
Approved for public release, distribution unlimited

13. SUPPLEMENTARY NOTES
The original document contains color images.

14. ABSTRACT
This issue of the WSTIAC Quarterly features an article on Future Combat Systems Small Unmanned Ground Vehicles Teleoperation Experiment Results and High Efficiency Nuclear Power Plants Using Liquid Fluoride Thorium Reactor Technology. Included the WSTIAC Directors Corner, List of Training Courses sponsored by WSTIAC are also included in this issue.

15. SUBJECT TERMS

16. SECURITY CLASSIFICATION OF:			17. LIMITATION OF ABSTRACT	18. NUMBER OF PAGES	19a. NAME OF RESPONSIBLE PERSON
a. REPORT **unclassified**	b. ABSTRACT **unclassified**	c. THIS PAGE **unclassified**	**UU**	**16**	

EXPANDING WSTIAC'S KEY DOD STRATEGIC AREAS

In 2007 the Weapon Systems Technology Information Analysis Center (WSTIAC) revealed the "WSTIAC 10" – ten strategic areas critical to the Department of Defense (DoD) in which WSTIAC provides focused support. Since this introduction, WSTIAC has offered enhanced expertise and information for these ten areas as they relate to the technological advancement of weapon systems.

Director's Corner

Recently, WSTIAC identified an additional area of strategic importance to the DoD: *Maritime Surveillance.* Maritime surveillance has been defined as the systematic observation of surface and subsurface sea areas by all available means for the purpose of locating, identifying and monitoring surface ships, subsurface vehicles including submarines and other vehicles in the maritime environment.[1] The methods of surveillance involve the systematic use of visual, aural, and electronic means and other sensors and detection technology to gather data and information about sea-borne vessels.

The challenges associated with maritime surveillance can be summarized simply by the recognition of the vast space that the maritime environment occupies compared to the size of current threats that US forces face. This enormous maritime environment not only includes different media (i.e., water and air) through which energy used by sensor and detection technology must propagate, but the environment is not static; it is dynamic. As threats evolve over the course of the 21st century, so too must the tools to detect, identify and monitor them in order for the US military to successfully carry out their defense mission.

Technological advancements have brought maritime surveillance to the forefront of important defense capabilities, and it was recognized as a critical area in which the weapon systems technology community could provide integral support. Technology that enables improved maritime surveillance has obvious strategic value, and thus WSTIAC offers enhanced expertise and capabilities in this key area. To learn how WSTIAC can assist you within the area of maritime surveillance or any of the other strategic areas, visit our website: http://wstiac.alionscience.com.

This issue of the *WSTIAC Quarterly* features an article on the increasingly important small unmanned ground vehicles (SUGVs). Ground robots have already demonstrated their value on the battlefield, and are expected to save soldiers' lives for years to come.

The second article in this issue provides important detail on emerging nuclear technology. While the system in the article is discussed at a level not limited to any single application, the evolution of nuclear power technology has potential implications in the defense industry.

John Weed, WSTIAC Director

WSTIAC's Key DoD Strategic Areas

- Power & Energy
- Lethality
- Command & Control
- Non-Lethal Weapons
- Weapon Systems & Munitions Readiness & Asset Visibility
- Target Identification & Engagement
- Asymmetric & Irregular Warfare
- IED Defeat
- Embedded Training Systems
- **Maritime Surveillance**
- Capabilities, Effectiveness & Requirements Analyses

[1] "Department of Defense Dictionary of Military and Associated Terms," Armed Forces of the United States, Joint Publication 1-02, April 2001 (Amended August 2009).

The WSTIAC Quarterly *is the current awareness publication of the Weapon Systems Technology Information Analysis Center (WSTIAC). WSTIAC, a Department of Defense (DoD) Information Analysis Center (IAC), is administratively managed by the Defense Technical Information Center (DTIC) under the DoD IAC Program. All data and information herein reported are believed to be reliable; however, no warrant, expressed or implied, is to be construed as to the accuracy or the completeness of the information presented. The views, opinions, and findings contained in this publication are those of the author(s) and should not be construed as an official Agency position, policy, or decision, unless so designated by other official documentation. The appearance of an advertisement, announcement, product/service review, or article in the* WSTIAC Quarterly *does not constitute endorsement by the DoD or WSTIAC.*

Inquiries about WSTIAC capabilities, products, and services may be addressed to

John Weed
Director, WSTIAC
973.770.0123
email: jweed@alionscience.com
url: http://wstiac.alionscience.com/

Robert Fitzgibbon
Bruce Dudley
Technical Inquiries
877.WST.USER
email: wstiac@alionscience.com

We welcome your input! To submit your related articles, photos, notices, or ideas for future issues, please contact:

WSTIAC
ATTN: Benjamin D. Craig
201 Mill Street, Rome, New York 13440

phone: 315.339.7019 • fax: 315.339.7107
email: wstiac@alionscience.com

Future Combat Systems Small Unmanned Ground Vehicle Teleoperation Experiment Results

Barry O'Brien
Jesse Kovach
US Army Research Laboratory
Adelphi, MD

INTRODUCTION

With the Army's Future Combat Systems (FCS) transformation effort well underway, one is hard-pressed to find a system or component that has not been rethought and redesigned in some way. This is especially true in unmanned vehicles, where all of the proposed platforms are being developed from scratch. Specifically, the Small Unmanned Ground Vehicle (SUGV) will be an all new platform, and unlike prior fielded man-portable robotic systems, the SUGV will be required to use a common radio for communicating with its operator and the FCS network environment.[1]

The radio that an unmanned vehicle uses to communicate with its operator can act as either an enabler or the limiting factor of the platform's performance. With poor performance and low usable bandwidth, the platform becomes little more than a very expensive remote-controlled car. However, with enough bandwidth and performance a platform can provide real-time intelligence, surveillance and reconnaissance (ISR) information to the people responsible for making decisions to act on it, which makes the unmanned vehicle an incredible asset to the warfighter.

The FCS program proposes to use the Joint Tactical Radio System (JTRS) Solider-Level Integrated Communications Environment (SLICE) radio to be the SUGV radio solution operating with the Soldier Radio Waveform (SRW). The FCS Network Analysis and Integration Laboratory (NAIL) conducted the initial experiments during the 2007 Command, Control, Communications, Computers, Intelligence, Surveillance, and Reconnaissance On-The-Move (C4ISR OTM) experiment. The radio was employed to tele-operate a SUGV-class platform using a prototype system called the Wearable Soldier Radio Terminal (WSRT). Working with NAIL representatives, Army Research Laboratory (ARL) engineers integrated the WSRT radios on to the existing PackBot®*† system, the first time that the radio, which was mandated by FCS to be on the SUGV, had been installed in a SUGV system, surrogate or otherwise. A series of experiments were then performed to examine the radio's performance, and further compared to the performance of the ARL radio solution.

This article briefly describes the integration effort that took place to allow the WSRT to control the ARL PackBot® system. It will then focus on performance results, comparisons with the ARL radio solution, and initial conclusions. Further information on these experiments can be found in the ARL Technical Report ARL-TR-4660.[2]

HARDWARE

Two different sets of radio hardware were used in this experiment. The first was an 802.11-based system that was implemented by ARL for use in the C4ISR OTM experiment.[2-5] The first system served as a baseline to measure our second system against, since characterization had already taken place. The second system was a WSRT radio system provided by the FCS NAIL.

WSRT Radio

The WSRT is a software definable radio capable of supporting both narrow and wideband waveforms. The WSRT is an internet protocal (IP)-based radio that provides six different SRW settings and operates in the ultra-high frequency (UHF) band at up to five watts (W) of transmit power. The objective was to evaluate a prototype WSRT system provided by ITT to the NAIL (production versions of the radio were to have improved specifications and different form factors). Of particular interest in this experiment is the WSRT's use of a communications protocol with a very high per packet overhead. The result is that only a certain number of packets can be sent per second, with minimal regard for the size of those packets. For the default settings of the WSRT, the maximum number of packets per second is 36 for small packets (less than 100 bytes) and 27 for large packets (greater than 1200 bytes). The low 33% increase in transmitted packets for such a large range in packet size points to a very high per packet overhead rate. This contrasts sharply with the 802.11 system, which is a data rate limited radio that only allows a certain amount of data to be sent per second, regardless of the number of packets that comprise the data.

PackBot® Payloads

The ARL ad hoc system was placed in a modular payload bay in the bed of the PackBot®. The payload bay interfaces to the robot through a payload breakout board developed at ARL. Mounted in the payload were a PC-104 style DC-DC voltage converter to power the ad hoc node router, and the router itself, removed from its plastic case to reduce its size. A high gain, flexible antenna originally in use on the PackBot® was mounted to the exterior of the payload so that the operational capabilities of the PackBot®, such as the ability to drive while inverted, were not sacrificed.

Packet level data was to be collected using the C4ISR OTM testbed's Data Collection and Analysis Tool (DCAT). DCAT is a customized packet sniffer that logs all network traffic for later analysis. For proper operation, DCAT needs to see all traffic on

http://wstiac.alionscience.com/quarterly

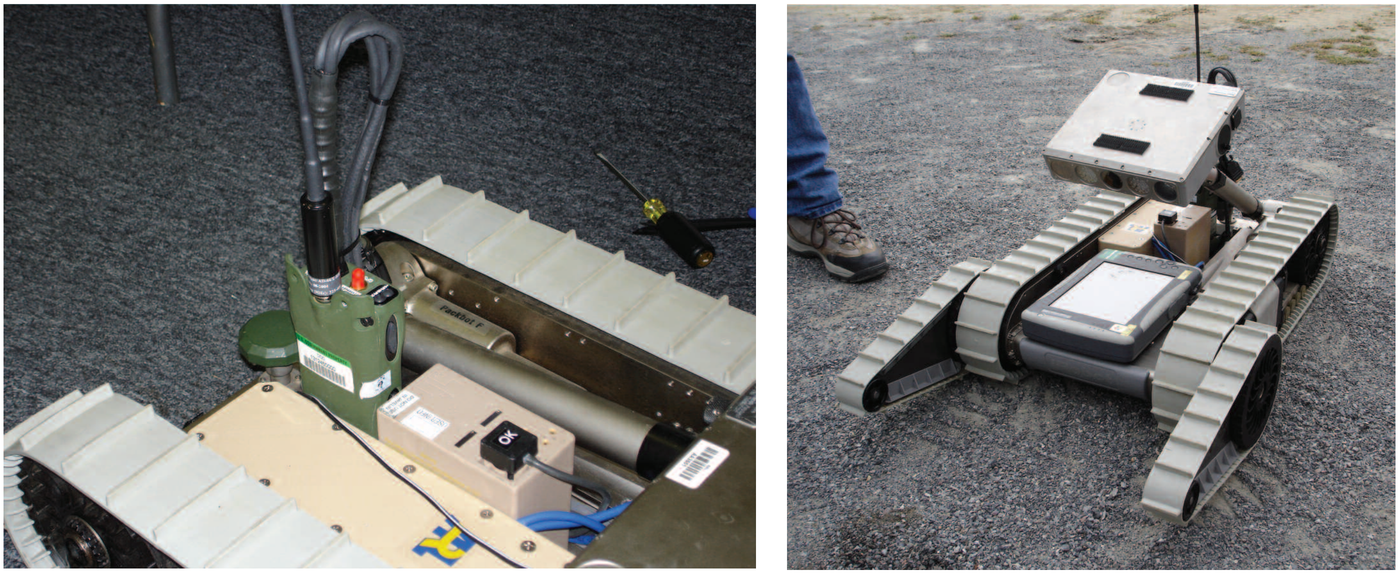

Figure 1. **WSRT integration onto PackBot® (left) with tablet PC for data collection (right).**

the platform. On larger vehicles, this is accomplished by using a high-end managed switch configured with an analyzer port that mirrors traffic from the other switch ports. This approach, however, is not practical for a small platform such as the PackBot®. Instead, we built a small payload containing a small five-port hub, and connected the robot to both the WSRT radio and a robot-mounted rugged tablet PC loaded with the DCAT software. Since a hub sends all packets to all ports, this configuration allowed DCAT to monitor the traffic between the robot and the radio.

Mounting the WSRT to the PackBot® chassis was difficult given the radio's form factor, which was intended for dismounted applications. The power and network connections exited from the bottom of the radio, while the antenna protruded out the top. So that the top mounted antenna maintained the appropriate upright position, the radio was secured to the side of the payload container using a hook-and-loop fastener (see Figure 1). The BB-2590 battery that powered the WSRT was also mounted with hook-and-loop fastener to the PackBot® chassis.

Figure 2. **ARL OCU modified to use WSRT.**

Operator Control Unit

ARL had previously designed a dismounted operator control unit (OCU) for use in the 2006 C4ISR OTM Capstone Experiment that was ruggedized to protect it from the abuses of dismounted field operations. The OCU consisted of a ruggedized tablet PC mounted in a custom metal frame that housed two joysticks used in robotic tele-operation. Mounted to the back of the frame was an 802.11 ad hoc node for communicating with the robotic assets.[3] The integration required to use the SRW radio with the existing OCU was minimal. The 802.11 radio was replaced with the WSRT and an additional battery was added to power it (see Figure 2).

SOFTWARE

ARL Software

The foundation of the ARL software suite is the Agile Computing Middleware (ACM) library, which provides discovery and point-to-point communications services using a transport-independent application programming interface (API). All applications and servers use ACM to communicate over the network. The ACM allows transport components to be integrated, tuned, and modified without requiring application-level changes.

A minor modification was made to the ACM library to allow applications to set the type of service (TOS) field, also known as the differentiated services code point (DSCP), in the IP packet header. The WSRT radio can operate in time division multiple access (TDMA) mode that essentially reserves a percentage of bandwidth for traffic in a single direction between a single pair of nodes, reducing negotiation overhead. When operating in this mode, the radio routes packets with a certain value in the TOS field over the reserved link. The video server, called MCVideoAgent, was modified to optionally set this flag for the video connection between the robot and the OCU. No other software was modified to use this option.

The only component installed on the OCU for this experiment was the CollectControl application, which allows users to connect to robots and other controllable devices, view video

http://wstiac.alionscience.com/quarterly

from the onboard cameras, and control the platform. CollectControl interfaces with the NewRobotAgent, PlatformPosture Server, and MCVideoAgent components on the robot through the ACM.

Video Compression Algorithms (Codecs)

MCVideoAgent and its companion CollectControl OCU application are implemented with a modular architecture that allows use of multiple video compression algorithms (codecs). Video codecs and codec parameters can be changed in the field by editing the video server's configuration file. ARL currently uses either the Motion JPEG (MJPEG) or MPEG-4 Part 2 compression algorithms. ARL uses the industry standard Independent JPEG Group (IJG) implementation of MJPEG and the ffmpeg implementation of MPEG-4.

Both codecs have their strengths and weaknesses.[2] ARL has noticed through informal testing that MJPEG often performs better than MPEG-4 over high bandwidth 802.11-based wireless networks due to MJPEG's ability to instantly recover from frame loss. However, bandwidth on the SRW radio is much more limited. ARL evaluated several different combinations of compression settings to determine what functioned best over the SRW link. Results of these tests are detailed later in this article.

EXPERIMENT RESULTS

Throughput Evaluation

After establishing initial connectivity between the OCU and the robot, ARL attempted to drive the robot using normal OCU settings and see what adjustments, if any, needed to be made.

The standard video settings used to control the robot are a resolution of 320 x 240 MJPEG at a requested frame rate of seven to eight fps. Previous experiments have shown these settings to be adequate for tele-operation.[3-5] Connection with the robot was successful at these settings, but it was evident from the choppy video that many video packets were being lost during transmission. This level of video performance is generally not considered acceptable to tele-operate the robot, so ARL lowered the resolution. Lowering the resolution to 160 x 120 MJPEG netted much better packet reception, receiving around six fps.

Two observations were made while troubleshooting this behavior. The first was that the WSRT radio at five W of output power was interfering with the joysticks on the ARL OCU. To address this issue, the min/max transmit power was reduced on both WSRT's to 100 mW, but it was unknown at that time how it would affect the range of communications. Secondly, it took approximately ten seconds after "release control" was pressed on the OCU screen to stop robot movement. It was determined that this was most likely due to network packet queuing occurring in the radios. Based on that, the "intranet queue size" parameter in the radios was changed from 1000 to four.

Once this basic level of connectivity and control was established, ARL attempted determine the limits of those parameters. The test plan evolved as more was learned about the limitations of the radios and observations were made of what was working and what was not. Thus, the results shown in the following section are of tests that may show useful data, but are not meant to be exhaustive, rigorous, or authoritative.

MJPEG Indoor Testing

The following tests were performed with the PackBot® system placed on blocks so that unanticipated movements would not be in any way destructive. The test consisted of first establishing video connectivity to the robot, then attempting to move the head and/or tracks of the robot and viewing the video stream while someone waved their hands in front of the cameras. This provided some qualitative feedback about both the control and streaming video transmission on the WSRT radios.

The first test was done using the baseline settings established above, namely a resolution of 160 x 120 using MJPEG with a compression factor (cf) of 40 (see Table 1). Further, the packet allocation algorithm operating on the WSRT radio was 100% carrier sense, multiple access (CSMA).

Table 1. **160 x 120 MJPEG, cf = 40, 100% CSMA.**

Frame Rate	Comments
1–2 fps	Control and video latencies acceptable
3 fps	Edge of acceptable latency (queue starts building up)
4 fps	Large latency (queuing), ~0.5 sec delay in control of head

After noticing the large packet latency during the four frames per second (fps) test above, ARL changed the maximum transmission unit (MTU) on the PackBot® from 1500 to 1300 in an attempt to get smaller packets across the network more frequently. However, after performing the evaluation again, it appeared to have no effect on the latency.

Next, the packet allocation algorithm on the radio was switched to 50% time division multiple access (TDMA), which effectively dedicates 50% of the bandwidth to the video stream from the robot to the OCU. The tests were performed once again using 160 x 120 MJPEG with cf=40 (see Table 2).

Table 2. **160 x 120 MJPEG, cf = 40, 50% TDMA.**

Frame Rate	Comments
1 fps	Control is acceptable (worse than 1 fps at preset using CSMA), but video good
2 fps	No change in control latency, but improvement in video (no latency other than standard delay)
8 fps	Video delay begins

The results so far were satisfactory, with the switch to 50% TDMA improving the control and video significantly. ARL then set out to determine the limits of the throughput of a higher resolution video stream, as resolution seemed to be our limiting factor. For this, the resolution was increased to 320 x 240, the standard operating resolution of the ARL PackBot® system, using the same MJPEG and TDMA settings.

Table 3. **320 x 240 MJPEG, cf = 40, 50% TDMA.**

Frame Rate	Comments
1 fps	Control hit/miss like prior test, video OK (80kb/s)
2 fps	Same as above, video stable
3 fps	Same as above
4 fps	Without driving: Control same, video good, driving = ~1 sec delay
5 fps	Would not go above 4.4 fps, same bitrate as 4 fps, ~3 sec of video delay

As can be seen, the control was suspect throughout the test, and the video throughput only got worse. It appears that the WSRT simply cannot support higher resolution MJPEG data using either 100% CSMA or 50% TDMA packet allocation schemes; there are not enough packet slots to handle both the packets required for tele-operated control and higher resolution video frames.

Packet Reduction Modifications

Some of the ARL software programs, for various reasons, generate small packets at relatively frequent intervals. On wired networks and 802.11 wireless networks, the per-packet overhead is small enough that these small packets are not a major concern. However, the WSRT radio has a much higher per-packet overhead, and it was thought that these small packets may be having an adverse impact on the performance of our control software over the WSRT link. There were two main sources of small packets that could be reduced: Group Manager "hello" packets, CollectControl teleoperation packets.

The Group Manager discovery system by default broadcasts a hello packet every two seconds. Presently, this information is simply printed to the screen, and no software makes use of it at the present time. It was determined that the hello packets could be turned off without any detrimental effect on the system, thereby cutting traffic by one packet per second on average (one packet every two seconds per node, for two nodes.)

CollectControl sends teleoperation (teleop) packets to the robot at variable intervals. Two types of packets are sent: mobility teleop packets containing platform translation and rotation rates, and pantilt teleop packets containing camera pan, tilt, and zoom rates. These packets are sent either twice a second or whenever the application detects that the joystick position (and therefore the associated movement or pantilt command) has changed. The joystick is polled at 25 Hz, so bursts of up to 50 packets per second (one mobility packet and one pantilt packet per sampling interval) could be generated for worst-case joystick movements. These bursts of packets caused increased latency on the radio. CollectControl was modified to put a configurable maximum on the rate at which teleop packets could be sent, and configured this maximum to be five Hz (ten packets per second.) This modification cut traffic by 0 to 40 packets per second depending on joystick movement patterns.

After these modifications were made, ARL estimated that average packet rates for commands and telemetry, not including video, were four packets per second from the robot to the OCU and four to five packets per second from the OCU to the robot.

Qualitative Control Test

After the packet reduction modifications were made to the ARL software and confirmed to be working, we decided to observe the control behaviors while driving the robot on the ground. In the authors' opinion, simulation and static testing can never give results as useful as simply getting a robot on the ground and making it move through a real environment.

For this test, we used the best combination of settings we had observed thus far: 160 x 120 MJPEG at six fps. This is substantially inferior to ARL normal PackBot® configuration, which operates at a higher resolution (320 x 240) and frame rate (greater than eight fps).

The test was to move the robot, driving via the streaming video, out of a trailer, down a set of stairs to the ground, moving away from the building a short distance, and then bringing it back up the stairs and into the trailer. Throughout the test, control lag was present, but it was consistent and thus manageable. The operator (one of the authors) commented that control was much smoother with the packet reduction modifications in place. Surprisingly, the system had little trouble with this test, aside from the obvious shortcomings of reduced resolution and frame rate. The system performed well exiting the trailer and outdoors.

An informal range test of the robot was performed so that any straight-line propagation issues with the radios could be identified. Using the same video parameters as the earlier control test (160 x 240 MJPEG at six fps), ARL attempted to drive the robot in a straight line from the development trailer down a dirt road towards the back of the range. At a distance of approximately 50 m, the connectivity to the robot failed. The SRW radios were examined, and it was determined that the failure was due to a feature of the SRW software that limits bandwidth when it believes it is near the edge of its communications range. The authors were told the only way to force the radios to remove the bandwidth limit was performing a hard restart on both radios. The radios were then restarted in place in an attempt to regain communications. ARL anticipated that the radios would regain communications at this point as the distance between them was not that great, and what was experienced was more of an anomaly. Communications were indeed reestablished, however we then tested if the bandwidth was still throttled by attempting to transmit 640 x 480 video at one fps and the system was unable to get a single frame through. This demonstrated that the radios either remained in the reduced bandwidth mode upon start up, or immediately sensed that they were at the edge of communications range and throttled bandwidth accordingly. Both scenarios were not ideal, given the line-of-sight between radios and relatively short distance.

MPEG4 Indoor Testing

Because of the identified issues using MJPEG frames at 320 x 240 with the WSRT, the authors attempted to perform the same tests using MPEG4, as it reduces the amount of large packets that needed to be sent over the network.

Presented below are the results using MPEG4 in the same manner as the MJPEG evaluations were performed above. That is, the robot was indoors on blocks in a static environment, with

Table 4. **160 x 120 MPEG4, bitrate = 150ks.**

Frame Rate	kBps	kbps	Comments
1 fps	5-10	40-80	Still images appear better quality than comparable MJPEGs, bad control lag.
2 fps	7-12	56-96	Control lag slightly better.
3 fps	9-16	72-128	Control lag slightly better. Suspect reason that control is getting better w/increase in frame rate is due to the way MPEG codec makes large frames for small fps when targeting a certain bitrate.
4 fps	14-25	112-200	Video still looks good (still better than MJPEG at this resolution, little delay), but control got jumpy and slightly laggy.
5 fps	16-28	128-224	Video was OK, control was good (better), but seems to hiccup when key frame goes across.
6 fps	21-25	168-200	Frame rate seems more stable, pretty good control.
8 fps	18-27	144-216	Pretty stable data rate especially with stills, hit or miss with control lag, but more miss than hit during movement, frame rate dropped to 6 fps.
10 fps	22-25	176-200	Consistent 0.5 sec video lag, video quality dropping. Frame rate is jumping around more (according to CollectControl). When lots of movement in the frame it gets temporarily blurry. Very noticeable control lag (comparable to 1–2 fps).

http://wstiac.alionscience.com/quarterly

hands being waved in front of the camera to introduce motion into the scene. The first results presented below are that of 160 x 120 MPEG4 operating at a target bitrate of 150 kbps. The data rate columns shown correspond to the byte and bitrate, respectfully, received by CollectControl.

The results in Table 4 point to MPEG4 video of static scenes that is clearer than corresponding MJPEG images, which contained more compression artifacts. However, this benefit is likely outweighed by the noticeable control lag, and the control hiccups and blurry video that come with movement in the image scene. Caused when the large key frame of the MPEG4 encoder comes through the system, these blurred images and inconsistent control lag at higher frame rates could be troublesome during tele-operation.

Per the test methodology used in the MJPEG tests, next the resolution was increased to 320 x 240 and evaluated at multiple frame rates.

Table 5 shows that as the frame rate increased on the MPEG4, control and video improved until motion was introduced into the scene. Even the slight motion caused by waving a hand in front of the camera from a short distance caused the video to become basically unviewable at the higher resolution of 320 x 240. This is a problem for a mobile robot system, as rarely will the scene viewed by the robot be static.

Table 5. 320 x 240 MPEG4, bitrate = 150k.

Frame Rate	kB/s	Comments
1 fps	4-9	Image more clear at this resolution, but blurry during movement. Control not bad, but during movement the video lost many frames and did not recover quickly. This may be that it is not passing packets over a certain size.
4 fps	11-18	Control is much better, but video has motion problems (blurry with movement) – video looks worse than 160x120 at 4 fps with movement.
8 fps	11-19	Video very poor with movement, control about the same.

Communications Range Evaluation

Following the throughput evaluations, outdoor range tests were performed using the WSRT-equipped PackBot® so a comparison could be made with the baseline 802.11-equipped PackBot® performance, both in head-to-head tests and against previously performed evaluations of the 802.11 ad hoc communication system.[3, 4]

MJPEG Outdoor Testing

Two driving scenarios were used outdoors. The first was a straight line-of-sight (LOS) path that took the PackBot® across an unobstructed sand clearing. The second was a non-line-of-sight (NLOS) path that put a metal building and a wooded mound between the PackBot® and the operator. These scenarios were designed to determine if output power of the WSRT had an effect on the absolute distance at which the system was able to be acceptably controlled. Thus, output power on the radios was iterated from 100 mW to five W. Further, per previous results, all tests were performed at a resolution of 160 x 120 using MJPEG with a target frame rate of six fps, and included all field fixes described above.

Finally, as a control measure, ARL attempted to run the same paths with the 802.11-based PackBot® system.

It is interesting to note that at full output power (five W), the WSRT radios actually performed worse than they did at less than half of that power level (two W), in both LOS and NLOS situations (see Table 6). The maximum distance achieved was 175 m in a LOS situation at two W of output power.

Alternately, the 802.11-based PackBot® was operational for such a distance that there was difficulty in accurately measuring its NLOS path length (see Table 7). This approximate distance corresponds to prior distance tests with this system, where straight line distances ranged from 193 m to 386 m, depending on the environment.[1, 2] These values represent a sizeable increase in the range and video resolution over the WSRT results.

Table 7. 320 x 240 MJPEG outdoor test results, 802.11.

802.11	Distance	Comments
LOS/NLOS	240 m+	Distance measured was straight line distance. Made 90 degree left turn out of LOS and continued acceptable operation for another ~100 m.

MPEG4 Outdoor Testing

The final test performed was to use MPEG4 encoding in an environment with more natural clutter than the fairly benign indoor environment used previously. It was anticipated that similar problems with movement within a scene would arise. To confirm the performance of MPEG4, the video encoding on the PackBot® was set to a bit rate of 100 kbps and the OCU attempted to display the video at 320 x 240 at 11 fps, which if operating correctly would provide video of rough equality to the standard MJPEG video settings used. The MPEG4 bitrate was lowered at this point from 150 kbps in an attempt to lower the latency some, as it was observed that we were still attempting to push too much data over the radio.

This resulted in much poorer video quality than the equivalent MJPEG settings, caused not by dropped packets so much as the lower bit rate resulting in unresolved video. Other contributors, which were speculative and could not be verified in the field, could have been a noisy camera (introducing noise due to bad ground connections) or a timing issue with the MPEG4 encoder. A further observation was that when driving the robot towards a

Table 6. 160 x 120 MJPEG outdoor test results, WSRT.

Output Power	Path	Distance	Comments
100 mW	LOS	137 m	Robot lost control but not video, but quickly regained control but lost video. Suspect SRW bandwidth throttling property.
100 mW	NLOS	108 m	None
1 W	LOS	140 m	None
1 W	NLOS	90 m	None
2 W	LOS	175 m	None
2 W	NLOS	156 m	Operators note that driving using the streaming video is easier than watching the robot, as the control delay appears more consistent with delayed video.
5 W	LOS	160 m	WSRT radio on the robot jostled loose from driving, causing communications to fail. Had difficulty reestablishing communications following reattachment.
5 W	NLOS	127 m	Eventually reestablished communications. Control unacceptable once behind the building.

http://wstiac.alionscience.com/quarterly

non-busy scene, such as a low horizon showing mostly white/blue sky with no trees, the video performance was great. However, as soon as the scene became dominated with busy things (less horizon, more trees), the video quality dropped very quickly.

CONCLUSION

The quantitative outdoor evaluations showed that the WSRT system consistently operated at a lower resolution, a lower frame rate and had a shorter communications range while utilizing a higher output power than the incumbent 802.11 system. Examining ping times on the different radio systems also showed a roundtrip time (RTT) delay of 120 ms for the WSRT radio with no network traffic, versus a one to two ms RTT for the 802.11 system. This imposes a network delay on all data before anything is actually transmitted, and only serves to exacerbate the control and video delays shown in the results above.

It is also important to note that all of the tests conducted were point to point; that is, network traffic only went between the robot to the OCU. It did not include any attempts to view video from two OCUs, or multiple radio hops, capabilities that the ARL system readily provides. The FCS NAIL engineer on this evaluation stated that attempting the multiple control to one robot scenario simply would not work due to the TDMA algorithm being used on the WSRT, as it only allows point to point communications at any given time.

The data presented above points to the conclusion that the current revision of the packet-rate limited WSRT radio does not appear ideal for tele-operation of robotic systems, as the small data packets required for control and telemetry information consume a large portion of the available network bandwidth, causing video quality to suffer significantly.

NOTES & REFERENCES

* PackBot is a registered trademark of the iRobot Corporation.
† The robot used was the iRobot PackBot Explorer.

[1] Capability Development Document for the Future Combat Systems, 20 July 2008, section 6.3.2.11.5.5.
[2] O'Brien, B., and J. Kovach, "Future Combat Systems (FCS) Small Unmanned Ground Vehicles (SUGV) Teleoperation Experiment Results," ARL-TR-4660, December 2008.
[3] O'Brien, B., D. Baran, and B. Luu, "Ad Hoc Networking for Unmanned Ground Vehicles: Design and Evaluation at Command, Control, Communications, Computers, Intelligence, Surveillance and Reconnaissance On-The-Move," ARL-TR-3991, November 2006.
[4] Zong, L., and B. O'Brien, "ARL Participation in the C4ISR OTM experiment: Integration and performance results," *Proceedings of SPIE Vol. 6562, Unattended Ground, Sea and Air Sensor Technologies and Applications IX*, April 2007.
[5] Gregory, T., J. Kovach, R. Winkler, and C. Winslow, "UGS, UGV and MAV in the 2007 C4ISR OTM Experiment," ARL-TR-4419, April 2008.
[6] Wearable Soldier Radio Terminal, www.cs.itt.com.

Comment on this article at wstiac@alionscience.com

High Efficiency Nuclear Power Plants Using Liquid Fluoride Thorium Reactor Technology

Albert J. Juhasz
NASA Glenn Research Center
Cleveland, OH

Richard A. Rarick
Rajmohan Rangarajan
Cleveland State University
Cleveland, OH

ABSTRACT

An overall system analysis approach is used to propose potential conceptual designs of advanced terrestrial nuclear power plants based on Oak Ridge National Laboratory (ORNL) molten salt reactor (MSR) experience and utilizing closed cycle gas turbine (CCGT) thermal-to-electric energy conversion technology. In particular conceptual designs for an advanced one gigawatt-electric (GWe) power plant with turbine reheat and compressor intercooling at a 950 K turbine inlet temperature (TIT), as well as near term 100 megawatt-electric (MWe) demonstration plants with TITs of 950 K and 1200 K are presented. Power plant performance data were obtained for TITs ranging from 650 to 1300 K by use of a closed Brayton cycle (CBC) systems code which considered the interaction between major sub-systems, including the liquid fluoride thorium reactor (LFTR), heat source and heat sink heat exchangers, turbo-generator machinery, and an electric power generation and transmission system. Optional off-shore sub-marine installation of the power plant is a major consideration.

INTRODUCTION

In meeting the increasing demand for electrical energy, today's global economies are faced with the dual problem of declining fossil fuel resources and climate change due to atmospheric accumulation of "greenhouse gases," principally carbon dioxide and methane.[1] An obvious solution to both issues would be a power generation process that does not require fossil fuels and also does not have any gas emissions. Among the proposed near-term alternative energy sources, the reliability and capacity factor of traditional nuclear fission power plants has steadily improved over the years to a level of approximately 92 percent, which is more than twice that of solar or wind. Additional benefits from nuclear power are possible, if investment in nontraditional nuclear power generation is undertaken. The inherent advantages of such advanced power generation schemes were recognized by the United States Congress when it passed the Energy Policy Act of 2005 (US 109th Congress, 2005). Development of advanced nuclear power plants was advocated under "Title VI—Nuclear Matters," and the goals of the "Generation IV Nuclear Energy Systems Initiative" were spelled out under Subtitle C "Next Generation Nuclear Plant Project" (NGNPP). In essence, these goals were to generate electric power for base load energy demands and to produce hydrogen as a new carbon-free fuel for vehicular transportation. Furthermore, Generation IV (Gen IV) power plants were to be highly economical, equipped with safety enhancements, have minimal waste, and be proliferation resistant. To meet these objectives a number of closed cycle gas turbine energy conversion systems either directly coupled to high temperature gas (cooled) reactors (HTGR), or indirectly coupled via intermediate heat exchangers (IHX) to liquid cooled reactors have been proposed.[2] For both configurations the gas turbine working fluid is helium (He), with power plant output ranging from tens of MW to GW levels.

A good comparison of the performance of power plants using either gas turbine (Brayton), or steam turbine (Rankine) energy conversion systems, in terms of the thermodynamic plant efficiency is shown in Figure 1, which was adapted from the literature, except for the abscissa coordinates altered from degrees fahrenheit to kelvin.[3] Due to the higher cycle temperature ratios enabled by the higher turbine inlet temperatures for gas turbine systems, a 50 percent increase in CCGT plant efficiency can be realized, when compared to the highest efficiency achievable with the steam cycle. Hence most Gen IV energy

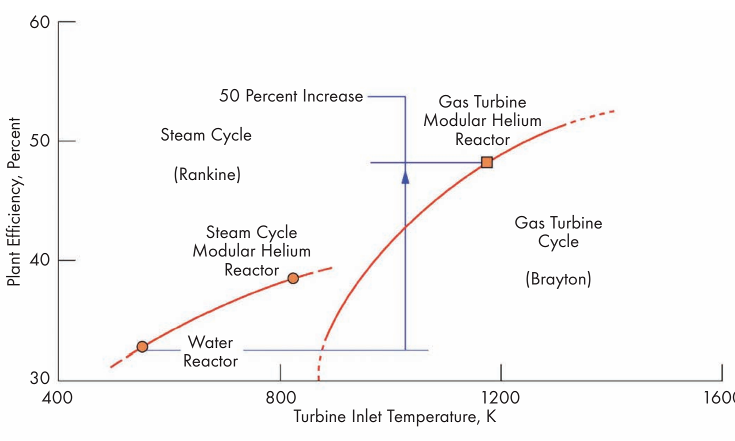

Figure 1. Energy conversion cycle comparision.[3]

This article was presented at the 7th International Energy Conversion Engineering Conference, August 2009.

http://wstiac.alionscience.com/quarterly

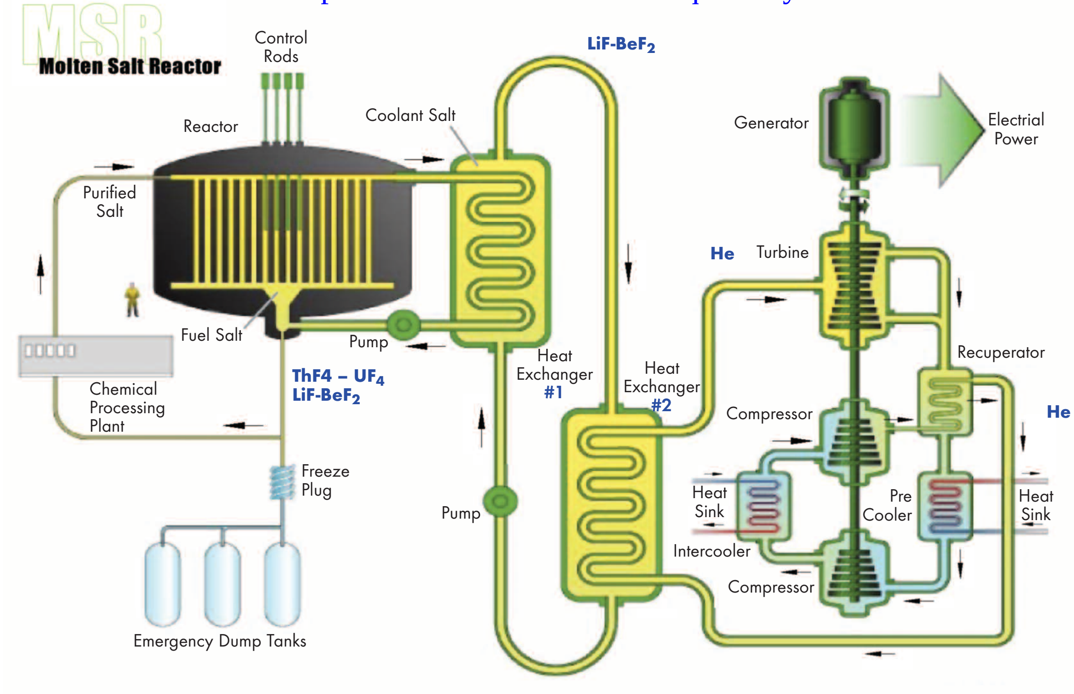

Figure 2. **ORNL's MSR/LFTR power plant with CBC conversion.**

conversion systems are based on the CCGT power cycle, also referred to as the closed Brayton cycle (CBC). For optimum rotor-dynamic performance, vertical orientation of the compressor-turbo-alternator machinery has been proposed.[4, 5] Acronyms like high temperature gas reactor (HTGR) or gas turbine modular helium reactor (GT-MHR) refer to the directly CBC systems, while CBC energy conversion via the very high temperature reactor (VHTR), MSR, or LFTR refer to indirectly heated cycles.[6, 7] Note that, due to the much higher heat transfer capability of liquid (molten) salt or metal, a VHTR can operate at higher outlet temperatures than the HTGR. The drawback is that additional investment in liquid-to-gas heat exchangers and circulating pumps must be made. However, such investment may be warranted if one considers that for a 1000 MWe plant generating power at 5¢/kW-hr ($50/MW-hr) each percent increase in plant efficiency translates into nearly $4.5 M in additional revenue.

Hence the objective of this paper is to examine how gas turbine power systems could use fission reactor heat sources based on the LFTR technology, developed at ORNL during the Molten Salt Reactor Experiment (MSRE) program.[8]

THE THORIUM FUEL CYCLE AND LFTR POWER PLANT

The thorium fuel cycle is based on a series of neutron absorption and beta decay processes initiated by neutron absorption and beta decay reactions starting with naturally occurring thorium-232 as the fertile material and the artificial uranium-233 ($_{92}U^{233}$) isotope as the fissile reactor fuel. Table 1 shows the three essential nuclear reactions.[9]

Table 1. **Thorium – uranium breeding cycle.**

1. $_{90}Th^{232} + {}_{0}n^{1}$ fi $_{90}Th^{233}$ + g (neutron absorption)
2. $_{90}Th^{233}$ fi $_{-1}b^{0} + {}_{91}Pa^{233}$ (beta decay – l= 22.3 min)
3. $_{91}Pa^{233}$ fi $_{-1}b^{0} + {}_{92}U^{233}$ (beta decay – l= 27 days)

The nuclear reaction indicated by step 1 shows, that a neutron absorbed by thorium-232 will bring about a transmutation to a new isotope, namely thorium-233 and emission of a gamma photon. Note that a logical source for the neutron required for absorption is a power producing fission reactor with the fertile thorium-232 contained in an annulus or blanket enveloping the reactor core. The thorium-233 isotope next (step 2) emits an electron (beta decay) as it rapidly transmutes to protactinium-233. With a half-life of only 22.3 minutes, over 99.9 percent of the $_{90}Th^{233}$ is converted into $_{91}Pa^{233}$ in four hours. In step 3 the protactinium-233 isotope undergoes a slow transmutation process by beta decay, with a half-life of 27 days, there is a storage requirement of about ten months for the protactinium-233 to decay to the fissile uranium-233.

Molten Salt Reactor Technology

The originators of this fluid fuel reactor technology were nuclear researches at ORNL, under the direction of Alvin Weinberg, who served as director of ORNL from 1955 to 1973.[10] The motivation for and the intended first application was in support of the Nuclear Aircraft project in the late 1940s under the Homogeneous Reactor Experiment (HRE) and the Aircraft Nuclear Propulsion (ANP) project. Reactor outlet temperatures near 1100 K (820°C) were achieved before the program was discontinued in 1961. However the technology acquired was shifted to a ground-based civilian version of a "meltdown proof" reactor, serving as heat source for both a steam power plant and later for a CBC.[8]

A schematic diagram of the ORNL-MSR gas turbine power plant is displayed in Figure 2. Shown on the left side of the figure is a graphite matrix moderated MSR reactor with fuel salt mixture (ThF_4-$U_{233}F_4$) being circulated by a pump through the core and to a primary (shell-tube) heat exchanger. Note that a parallel loop permits part of the fuel salt to be diverted to a processing plant and reintroduced into the core as purified salt. As one of the unique safety features, a melt-plug at the reactor bottom would permit the reactor fluid fuel to be drained into subcritical dump tanks, located in a underground storage facil-

ity, should the fuel salt temperature exceed a preset limit. A second pump circulates the liquid heat transfer fluid ($LiF-BeF_2$) through an intermediary heat exchanger where the helium working fluid is heated to turbine inlet temperature. The high pressure-high temperature helium is shown to flow through two parallel turbines which drive two intercooled series compressors and the electric power generator, all mounted on the same shaft. The turbine exhaust flows pass through the hot side of a recuperator where thermal energy is transferred to the high pressure compressor discharge flow before entering the water cooled heat sink heat exchanger (HSHX) which lowers the working fluid temperature to the value required by the LPC (low pressure compressor) inlet condition. The compressor raises both pressure and temperature of the He working fluid before the fluid is cooled back to near inlet temperature by the intercooling He-water heat exchanger. Due to the lower temperature at the inlet of the high pressure compressor (HPC), the compressor work will be reduced significantly, thus allowing more shaft power for the generator and thereby leading to higher plant efficiency. As a final step in completing the circuit, the He working fluid exiting the high pressure compressor enters the cold side of the recuperator where it is preheated by the turbine exhaust stream. The helium then enters the secondary heat exchanger where it is heated to the turbine inlet temperature requirement as explained above.

Although not shown in the schematic, reactor core heat can also be used for H_2 production by processes like high temperature electrolysis of water, or the water gas shift reaction. Thus all of the objectives set forth under the Energy Policy Act of 2005 could be accomplished with advanced nuclear technology as represented by MSR or LFTR.

Technological Advantages of LFTR Power Plants

Compared to traditional nuclear reactors which "burn" the fissile uranium isotope U_{235} the LFTR uses fissile U_{233} which is derived from Th_{232}. But whereas U_{235} constitutes only 0.7 percent of mined natural uranium, practically all of the thorium can be converted to U_{233}, and no processing for enrichment is needed. As will be shown in a later section of this paper, at turbine inlet temperatures of 1200 K closed cycle gas turbine thermal energy conversion efficiency, $?_t$, of over 50 percent can be attained, as compared to a 30 to 35 percent efficiency for currently operating steam turbines plants with inlet temperatures of approximately 570 K (300°C). Thus a factor of three hundred times as much output electric power per unit mass of raw fuel ore (uranium oxide (U_3O_8) versus Thoria (ThO_2)) can be obtained via the thorium fuel cycle with closed cycle gas turbine energy conversion. As a result fission fragment waste products are reduced by a commensurate amount, and their radioactivity would decay to background levels in less than 300 years, as contrasted to over 10,000 years for currently used reactors, thus obviating the need for long term storage, such as at Yucca Mountain. The thermal spectrum LFTR concept is inherently safe, with a negative temperature coefficient of reactivity, thus making a "core meltdown" due to loss of coolant impossible. Since the fuel is a pumped liquid solution of $LiF-BeF_2-UF_4$, refueling can be accomplished without reactor shutdown. The fissile fuel can also be made "proliferation resistant" by permitting it to be contaminated (denatured) with small amounts of U_{232} to increase its dose rate which would greatly reduce its unshielded exposure time and greatly increase detectability.

With thorium ores, such as Monazite, being four times more abundant in the earth's crust than uranium ores, over 60 percent of the world's resources are located in the following democratically governed countries: Australia (18 percent), United States (16 percent), India (13 percent), Brazil (nine percent), and Norway (five percent). Thus future global energy demands could be met by these thorium sources for over several tens of millennia.

CONCEPTUAL DESIGN MODELING OF GAS TURBINE LFTR NUCLEAR POWER PLANTS

Having established that closed cycle gas turbine power plants with both directly or indirectly supplied thermal energy from nuclear heat sources would best meet the NGNPP-Gen IV power plant requirements, an author-generated CBC code previously used in the modeling of space and planetary surface power systems was modified to meet the modeling requirements of terrestrial nuclear power plants.[11-14] Special emphasis was placed on incorporating the two series heat exchanger requirements of LFTR reactors as exemplified by ORNL MSRE technology.

Furthermore the provision for treating CBC compression and turbine expansion processes as composed of separate incremental series steps allowed for realistic modeling of power systems with compressor intercooling and/or turbine reheat options. Since cycle reject heat and intercooling heat transfer is accomplished via gas-water heat exchangers, the space radiator heat rejection sub-routines were bypassed in the modeling computations. Allowing for the working fluid passing through heat exchangers on the cycle hot side, recuperator, compressor intercooler and heat sink, the cycle pressure drop was set at four percent. Thus the turbine overall turbine pressure ratio for up to three series machines was 96 percent of the overall pressure ratio produced by the compressors. Provision was added to compute and display local pressure and temperature state points along the system schematic diagrams for modeling simulations for different cycle configurations, TITs and power output levels. A list of key input values which were kept constant is shown in Table 2.

Table 2. **Key cycle input parameters.**

Compressor Inlet Temperature (TIC), K	300
Cooling Water Temperature, K	288
Reactor Heat Loss, percent	1.0
Polytropic Efficiency–Compressor, percent	86
Polytropic Efficiency–Turbine, percent	92
Recuperator Effectiveness, percent	95
Intercooler HX Pressure Loss, percent	0.5
Reheat HX Pressure Loss, percent	0.8
Turbine Pressure Ratio Fraction, percent	96
Generator Efficiency, percent	98

Several conceptual power plant cycle configurations were modeled using the code briefly described above. As shown in Figure 3, the first of these is for a 1000 MWe power plant with turbine reheat and compressor intercooling (availability of water cooling reservoirs assumed), with a TIT of 950 K. With three series turbines and compressors, and the required heat exchangers on the hot side and cold side of the cycle, a fairly convolut-

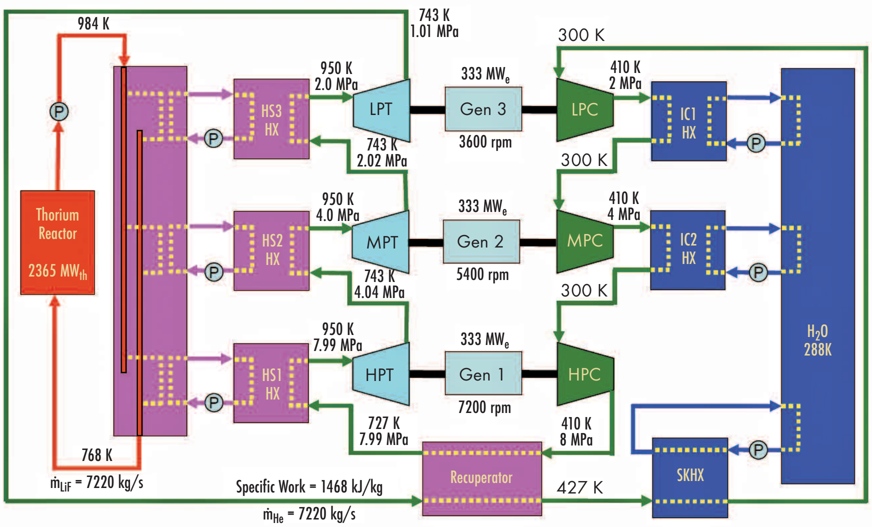

Figure 3. Schematic of one GW liquid fluoride reactor power plant with 950 K turbine reheat and compressor intercooling. Plant efficiency is approximately 42 percent.

ed cycle schematic was analyzed. Note that the total He mass flowrate was only about 681 kg/s for this three series turbomachine configuration with an overall pressure ratio of eight, with each stage ratio of two. The specific work parameter of 1468 kJ/kg expresses the ratio of total power output of 1000 MWe = 10^6 kJ/s to 680 kg/s. This flowrate is only a third of the over 2100 kg/s that would have been required for accomplishing the same power output with one large single compressor and turbine and the resulting specific work for this case would be less than 500 kJ/kg. So the system complexity is offset somewhat by much smaller rotating machinery and heat exchanger size. However another drawback is that, due to the cascading pressure levels the turbo-generator speeds (in rpm) optimize at 7200 for the HPT, 5400 for the MPT and 3600 for the LPT. This would require speed reducer transmissions for changing the intermediate and high pressure turboset speeds to 3600 rpm, for generation of 60 Hz electric power via two pole alternators.

The reactor thermal power is shown to be 2365 megawatt-thermal (MWt), which indicates a plant thermal efficiency of 42.3 percent. Even after subtracting the approximately three MWe for combined pump power requirements the plant efficiency is still above 42 percent for the 950 K TIT, requiring a reactor outlet temperature of under 990 K, assuming high effectiveness heat exchangers. Of course, just like for the ORNL MSR system, the primary reactor fuel-coolant is uranium tetrafluoride ($U_{233}F_4$) which may also contain LiF-BeF_2 eutectic in solution. The secondary heat exchanger fluid is LiF-BeF_2 liquid salt with a melting point of approximately 630 K.

The next cycle analyzed, shown in Figure 4, has been greatly simplified by removing the reheat feature, but keeping the three series intercooled compressors. The TIT is still 950 K, but the output power level is reduced to 100 MWe. Note that the overall pressure ratio for this system is approximately 2.21 (i.e., 2.08 MPa: 0.94 MPa). Even though there is no ‘reheat’, the

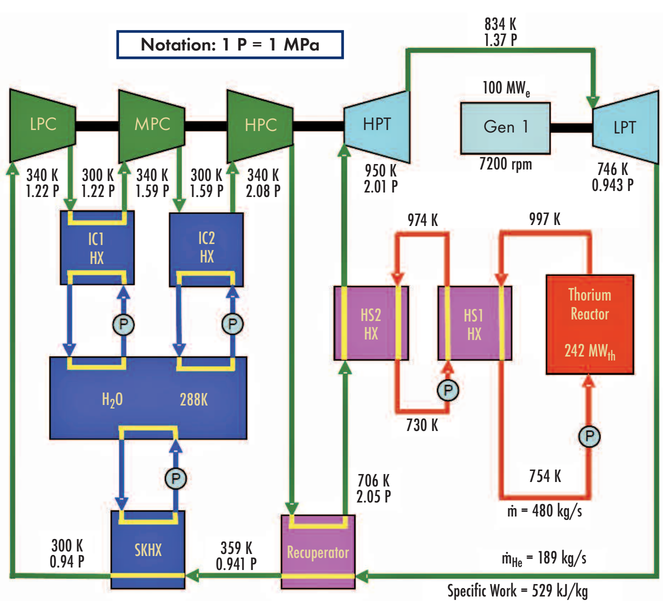

Figure 4. Schematic of 100 MWe liquid fluoride reactor power plant with 950 K turbine (no reheat) and compressor intercooling. Plant efficiency is approximately 41.3 percent.

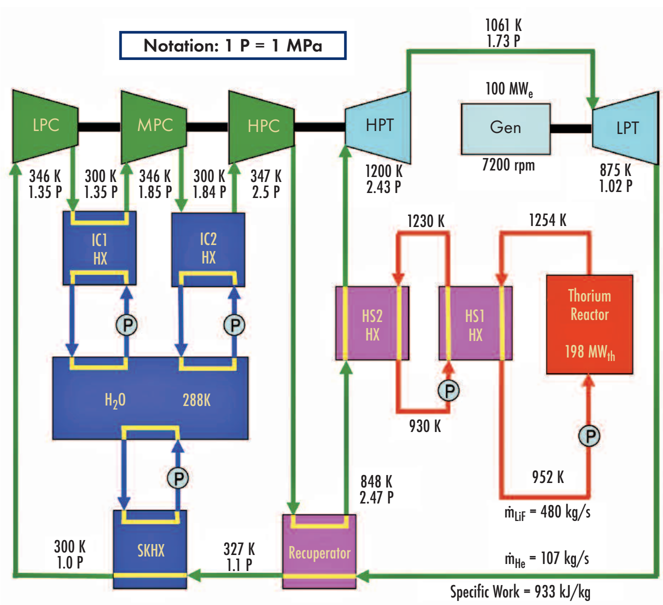

Figure 5. Schematic of 100 MWe liquid fluoride reactor power plant with 1200 K turbine (no reheat) and compressor intercooling. Plant efficiency is approximately 50.5 percent.

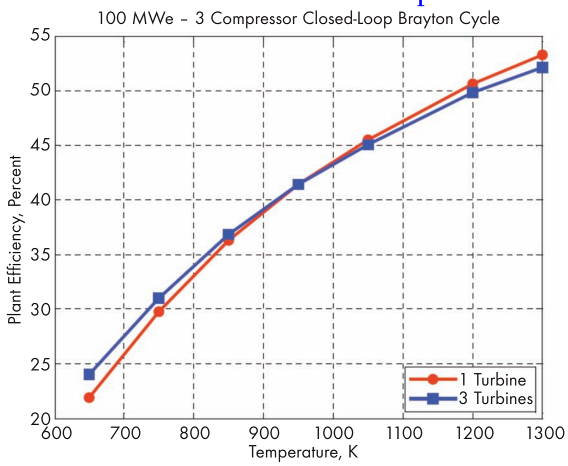

Figure 6. Power plant efficiency as a function of turbine inlet temperature for only intercooled (one turbine) and intercooled + reheated (three turbines) – 100 MWe CCGT power plant.

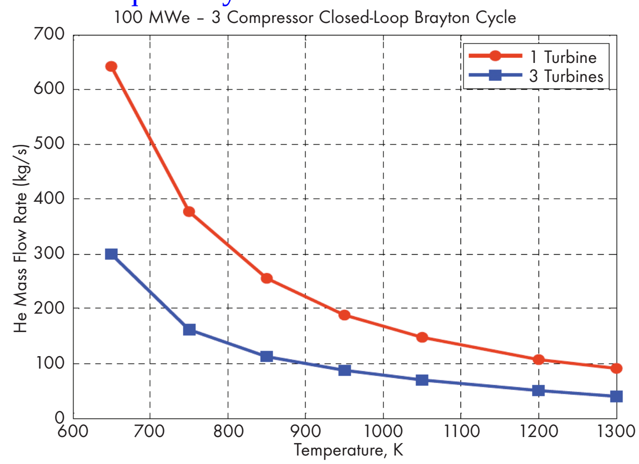

Figure 7. Power plant mass flowrate as a function of turbine inlet temperature for only intercooled (one turbine) and intercooled + reheated (three turbines) – 100 MWe CCGT power plant.

total turbine expansion work is split into two sections. The high pressure turbine (HPT) work is dedicated to driving the three series compressors with intercooling after the first and the second stage. The output of the low pressure turbine (LPT) at a TIT of 834 K is used to drive the 100 MWe generator. Although the turbine speed still optimized at 7200 rpm, higher power output levels with higher machine diameters would lead to optimum turbine speeds near 3600 rpm. But to design a 3600 rpm turbo-generator for a 100 MWe output the operating pressure levels could be reduced, albeit the turbomachine diameters would thereby need to be increased.

Note, that even without reheat the plant thermal efficiency only dropped about one percent. Compared to Figure 3, the number of hot side heat exchangers has been reduced from four to two. Such beneficial results with intercooling only were also pointed out in the reference literature.[15] Note that the specific work parameter has decreased to about 530 kJ/kg. This is indicated by the relatively high He mass flowrate requirement of 189 kg/s for this 100 MWe power output, when compared to the 681 kg/s mass flow for the 1000 MWe case of Figure 3. The primary and intermediate heat exchanger mass flows were computed on the basis of thermal capacity and density of the respective liquid fuel ($U_{233}F_4$) and $LiFBeF_2$ heat transfer fluids.

As shown in Figure 5, the last case analyzed was for a 100 MWe power output with the intercool only option. But the TIT was increased to 1200 K, thus providing a cycle temperature ratio of four. For this higher temperature ratio the plant thermodynamic efficiency increased to 50.5 percent and the overall optimum pressure ratio to 2.5. The specific work parameter almost doubled to 933 kJ/kg. This is as also reflected by the reduced He mass flowrate of 107 kg/s. Note also that the high pressure turbine exit temperature, which is also the inlet temperature for the low pressure turbine, increased from 834 K for the case discussed in Figure 4 to 1061 K for this higher TIT.

The higher plant thermal efficiency and specific work values, coupled with lower working fluid mass flowrate requirement, reinforce the fact that higher peak cycle temperatures enabled by advances in high temperature materials technology are the key to achieving economies in lower heat input requirements and lower component sizes. These promising trends augur well for rewards in the future if required investments are made in the present.

The results of a systematic increase in TIT from 650 K to 1300 K for intercooled only and intercooled + reheated gas turbine systems are shown in Figures 6 and 7, respectively. The first case, illustrated by the red curves, represents configuration of three series compressors and a single turbine.

The second case, illustrated by the blue curves, is representative of the three reheated series turbines plus three series intercooled compressor case, as shown in Figure 3. The dramatic increase in power plant thermal efficiency from the low 20's percent range for a TIT of 650 K, to over 53 percent at a TIT of 1300 K is shown in Figure 6. For the change in turbine inlet temperature shown the optimum pressure ratios increase from about 1.8 to 2.5 for the intercool only case. But for the intercool + reheat case the optimum pressure ratios increase from about 2.8 to near 8.0 over the same temperature range. Due to the higher pressure ratios, the isentropic compressor efficiencies are lower for the same polytropic value of 86 percent as shown in Table 2. This explains why the efficiency values for the intercooled only configuration surpass those for the intercool + reheat at the high turbine inlet temperatures. But, regarding total helium mass flowrate, Figure 7 shows that while the mass flow decreases by a factor of approximately six over the temperature range, the three turbine intercool + reheat configuration requires less than half the mass flow of the intercool only option. Since turbo-machine and heat exchanger size at the same operating pressure is proportional to working fluid mass flow, having larger sized components is the cost for reduction in system complexity offered by the single turbine intercool only option.

PLANT SUB-MARINE BASING AND HIGH VOLTAGE DC POWER

Although proposed here only in conceptual form with detailed designs to be generated at some future time, an LFTR-CBC power plant could be based offshore in a large submarine pressure vessel and the three phase alternating current (AC) power generated could be transformed to high voltage (HV) before rectification-conversion to HV direct current (DC) and trans-

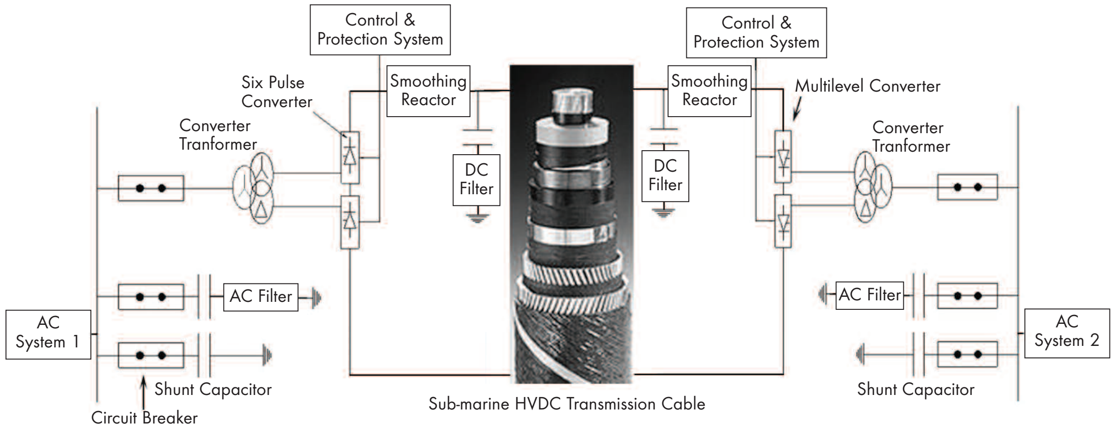

Figure 8. **Possible wiring for HVDC power transmission between source and load.**

mission via submarine cables to users in coastal regions. A preliminary electrical wiring scheme for power output from two parallel turbo-generators is shown in Figure 8.

The generator employed for the conversion process is an AC synchronous generator. The generated AC voltage is converted into DC voltage using a rectifier. A converter transformer is employed to step up the generated voltage to the necessary transmission voltage level. The converter transformer has two secondary windings, a delta and a Y-winding. This construction facilitates a 12-pulse rectification in the rectifiers. The construction of the converter transformer also suppresses the fifth and the seventh harmonic in the system. The DC voltage output from the AC-DC rectifier has very low ripple and hence low losses. Smoothing reactors are employed to reduce ripples from the system in conjunction with DC. The layout of a HVDC transmission system is shown in Figure 8. The mechanical energy filters. This improves the power quality of the transmitted power. The smoothing reactor, DC filter also act as protective devices and reduce the current surges in the system, in case of a fault. The smooth, filtered DC voltage is transmitted via submarine HVDC transmission cable. The transmitted DC has to be converted back to AC voltage for transmission and distribution purposes. The DC is converted into AC by employing a low loss, high efficiency multilevel converter. The inverted voltage is stepped up or down depending on the voltage on the terrestrial grid. The layout shows the other protective devices in the system. Some obvious advantages of a HVDC over HVAC transmission system are:

1. Economically cheaper—two cables only
2. Efficiency as the system losses are lower
3. Reliability—underground cable location
4. Security—buried or under-ground cables are less prone to sabotage

The offshore basing of nuclear power plants would also make them more acceptable for location within a few miles of metropolitan centers.

CONCLUDING REMARKS

Conceptual designs for ground-based gas turbine energy conversion power plants with advanced nuclear fission reactor heat input were analyzed using an author generated code with the capability to model gas turbine power systems with compressor intercooling and/or turbine reheat provisions. It was shown that, given high quality heat exchanger and turbomachine technology with 1200 K inlet temperature, power plants with a thermodynamic efficiency of 50 percent could be constructed.

In particular a nontraditional nuclear fuel, namely uranium-233, derived from natural thorium, nuclear power plants using a liquid fluoride thorium reactor would offer great benefits for ensuring future energy supplies, reduction of adverse climate effects due to greenhouse gas emissions, and invigoration of the world wide economy. With the inherently higher proliferation resistance of the thorium fuel cycle LFTR's meet the requirements of the Gen IV nuclear power plants as spelled out in the Energy Policy Act of 2005.

As confirmed by an author generated CBC code, even without the complexity of turbine reheat cycles, using intercooled only option, at least 50 percent of the thermal energy from LFTRs could be converted by gas turbine driven generators (operating at approximately 1200 K turbine inlet temperature) for electric power production during peak demand periods. Both thermal and electrical energy would be available during off-peak periods for hydrogen production by elevated temperature electrolysis of water or chemical processes such as the water gas shift reaction. This approach would both supply electric power by using environmentally clean nuclear heat which does not generate greenhouse gases, and it would also provide a clean fuel for the future, when, due to increased global demand and the decline in discovering new deposits, our supply of liquid fossil fuels will have been used up within the next 30 to 50 years, as predicted by the Hubbert model and confirmed by other global energy consumption prognoses.

The thermal spectrum LFTR concept is inherently safe, with a negative temperature coefficient of reactivity, thus making a core meltdown due to loss of coolant impossible. Since the fuel is a pumped liquid solution of $LiF\text{-}BeF_2\text{-}UF_4$ refueling can be accomplished without reactor shutdown. The fissile fuel can also be made proliferation resistant by permitting it to be contaminated (denatured) with small amounts of U_{232} to increase its dose rate which would greatly reduce its unshielded exposure time and greatly increase detectability. With thorium ores, such as Monazite, being four times more abundant in the earth's crust than uranium ores, over 60 percent of the

http://wstiac.alionscience.com/quarterly

world's resources are located in the following democratic countries: Australia (18 percent), United States (16 percent), India (13 percent), Brazil (nine percent), and Norway (five percent). Thus future global energy demands could be met by these thorium sources for over several tens of millennia.

ACKNOWLEDGMENTS

This work was conducted at NASA Glenn Research Center's Thermal Energy Conversion Branch and Cleveland State University (CSU). Any opinions expressed are those of the authors and do not necessarily reflect the views of NASA, CSU, or the Department of Energy.

REFERENCES

[1] Hubbert, M. K., "Nuclear Energy and the Fossil Fuels," Publication No. 95, Shell Development Co. – Exploration and Product Research Division, Houston, TX, June 1956.

[2] Richards, Matthew B., et al: "The H2-MHR: Nuclear Hydrogen Production Using the Modular Helium Reactor," Paper 5355 of Proceedings of the ICAPP '05, Seoul, Korea, May 15-19, 2005. US 109th Congress PUBLIC LAW 109–58 "Energy Policy Act of 2005," August 8, 2005.

[3] LaBar, Malcolm P., "The Gas Turbine–Modular Helium Reactor: A Promising Option for Near Term Deployment," General Atomics Report GA–A23952, April 2002.

[4] Zhao, H., and P. F. Peterson, "Optimization of Advanced High Temperature Brayton Cycles with Multiple Reheat Stages" 11th, International Topical Meeting on Nuclear Reactor Thermal-Hydraulics (NURET-11). Popes' Palace Conference Center, Avignon, France, October 2-6, 2005.

[5] Kodochigov, N. G., et al: "Development of the GT-MHR Vertical Turbomachine Design," 4th International Topical Meeting on High Temperature Reactor Technology, September 2008, Washington, D.C., USA.

[6] Baxi, C. B. et al: "Evaluation of alternate power conversion designs for the GT-MHR," 3rd International Topical Meeting on High Temperature Reactor Technology, Johannesburg, South Africa, October 1-5, 2006. Published in Nuclear Engineering and Design, HTR–2006.

[7] Baxi, C. B. et al: "Development of the GT-MHR Turbo Machine," Proceedings of the ASME Turbo Expo 2009, June 8-12, 2009, Orlando, FL.

[8] Engel, J. R., et al: "Conceptual Design Characteristics of a Denatured Molten-Salt Reactor with Once-Through Fueling," ORNL/TM-7207, July 1980.

[9] Glasstone, S., and A. Sesonske, "Nuclear Reactor Engineering" 3rd ed., D. Van Nostrand, Princeton, NJ, 1967.

[10] Briant, Raymond C., and Alvin M. Weinberg (1957). "Molten Fluorides as Power Reactor Fuels" (PDF). Nuclear Science and Engineering; 2, 797-803. http://www.energyfromthorium.com/pdf/NSE_moltenFluorides.pdf. (Retrieved on 2008-05-18)

[11] Juhasz, A. J., "Analysis and Numerical Optimization of Gas Turbine Space Power Systems with Nuclear Fission Reactor Heat Sources" Doctoral Dissertation, Cleveland State University, May 25, 2005.

[12] Juhasz, A. J., and J. T. Sawicki, "Lunar Surface Power Systems with Fission Reactor Heat Sources," NASA/TM–2005-214003, November 2005.

[13] Juhasz, A. J., "Multi-Megawatt Gas Turbine Power Systems for Lunar Colonies," NASA/TM–2006-214658, December 2006.

[14] Juhasz, A. J., "Heat Transfer Analysis of a Closed Brayton Cycle Space Radiator," NASA/TM–2007-215003, August 2007.

[15] Frutschi, H. U., "Closed Cycle Gas Turbines–Operating Experience and Future Potential," 1st ed. 2005; ASME, Three Park Avenue, New York, NY 10016.

Comment on this article at wstiac@alionscience.com

WSTIAC Directory

WSTIAC DIRECTOR
John L. Weed
100 Valley Road, Ste 102
Mount Arlington, NJ 07856
973.770.0123; Fax: 973.770.1808
Email: jweed@alionscience.com

WSTIAC DEPUTY DIRECTOR
Stephen E. Ashford
50 West Corp Center
3975 Fair Ridge Drive, Ste 320 South
Fairfax, VA 22033
703.259.5238
Email: sashford@alionscience.com

DEFENSE TECHNICAL INFORMATION CENTER
Attn: IAC Program Office (DTIC-I)
8725 John J. Kingman Road, Ste 0944
Fort Belvoir, VA 22060-6218
703.767.9120; Fax: 703.767.9119
Email: iac@dtic.mil
URL: http://iac.dtic.mil/

TECHNICAL INQUIRIES
Robert Fitzgibbon
Bruce Dudley
201 Mill Street
Rome, NY 13440
877.WST.USER; Fax: 315.339.7002
Email: wstiac@alionscience.com

TRAINING COURSE COORDINATOR
Mary Priore
201 Mill Street
Rome, NY 13440
315.339.7135; Fax: 315.339.7002
Email: mpriore@alionscience.com

WSTIAC
Weapon Systems Technology
Information Analysis Center
201 Mill Street
Rome, NY 13440-6916

Prsrt Std
US Postage
Paid
Utica, NY
Permit No. 566

Please update...
and verify your subscription information at: **http://wstiac.alionscience.com/certify**

Inquiry Line/Ask the Experts
877.WST.USER

Free Subscription
http://wstiac.alionscience.com/subscribe

What Did You Think of Our Special Issue on Power and Energy?

This year, we were pleased to offer a special edition of the *WSTIAC Quarterly* devoted entirely to DoD power and energy initiatives. We hope you enjoyed this issue and invite you to take a few minutes to complete our quick 7-question survey.

Take our survey!

http://wstiac.alionscience.com/wqenergysurvey

Expanded Content Available Online

Download the online version of this special edition and read the expanded TechSolutions article starting on page 48.

http://wstiac.alionscience.com/wqenergy